FEBS 28876 FEBS Letters 576 (2004) 381–386

Role of the C-terminal region of mouse inducible Hsp72 in the recognition of peptide substrate for chaperone activity

Michiko Ohno, Naofumi Kitabatake, Fumito Tani*

Division of Food Science and Biotechnology, Graduate School of Agriculture, Kyoto University, Goka-sho, Uji, Kyoto 611-0011, Japan

Received 24 August 2004; accepted 16 September 2004

Available online 28 September 2004

Edited by Jesus Avila

Abstract Here, we produced the C-terminal truncation variants of mouse inducible heat shock protein 72 (Hsp72) to elucidate the regulatory role of the C-terminal helical lid of Hsp70 for substrate recognition. All of the truncation variants containing the substrate binding domain bound a short-length peptide substrate CLLLSAPRR. When a large mass reduced carboxymethyl α-lactalbumin (RCMLA) as a substrate was used in gel filtration experiment, we observed the complex formation only for the truncation variants containing the long α-helix C in the helical lid. However, RCMLA binding occurred even for the variants lacking α-helix C when their C-terminal region was anchored onto a solid phase. Together with the finding that helix C is involved in the self-association of Hsp70, our present data suggest that the C-terminal region of Hsp70 modulates the substrate recognition and its kinetics may be substrate-mass dependent.

Keywords: C-terminal helical lid; Heat shock protein 70; Peptide binding; Substrate mass; Truncation variant

1. Introduction

Heat shock protein (Hsp) 70 is one of the molecular chaperones that are expressed constitutively or in response to several types of stress, including heat shock, oxidative stress, glucose deprivation, and exposure to toxins and heavy metals [1–4]. Hsp70s are known to assist a variety of cellular processes such as protein folding, assembly and disassembly of multimeric proteins, protein translocation across membranes, protein degradation and signal transduction [2–4].

The molecular chaperone Hsp70 is basically composed of three structural domains [5]. The N-terminal 44 kDa segment that contains the adenosine nucleotide binding site displays a weak intrinsic ATP-hydrolytic activity [6,7]. The structure of this domain is similar to the structures of hexokinase and actin [7–9]. The adjacent 18 kDa segment has been shown to bind peptide substrates [10]. The X-ray crystallographic study revealed that the peptide binding domain consists of a β-sandwich structure made up of eight β-strands and loops [11]. The channel to which peptide substrates are bound is covered with a compact lid-like structure made up of α-helices that are followed by a disordered flexible tail [11]. Recently, Chou et al. [12] reported that the folding pattern of α-helices in the lid structure of rat Hsc70 differs from that of DnaK. The region of DnaK in the lid structure is composed of four helices, αB–αE, whereas the equivalent region of rat Hsc70 adopts a helix-loop-helix conformation.

A variety of peptides and nascent polypeptide chains have been shown to be substrates of the C-terminal peptide binding domain of Hsp70 [13,14]. In general, Hsp70 preferentially binds hydrophobic peptides. A minimum peptide length of seven residues is required for optimal binding to BiP, the ER-located Hsp70 [15]. It has been proposed that BiP preferentially binds peptides containing hydrophobic residues in alternating positions [16]. Hsp70 also forms a stable complex with unfolded proteins, such as reduced carboxymethylated α-lactalbumin (RCMLA), a thermally unstable mutant of staphylococcal nuclease, and apocytochrome *c* [17–19]. DnaK binding sites in protein sequences were found to occur statistically in every 36 residues [20]. Using a leucine-rich octapeptide and RCMLA, Hu and Wang reported that the C-terminal 10 kDa fragment appears to play a role in complexing with RCMLA [21]. However, it remains to be elucidated how the C-terminal region of Hsp70 is involved in the recognition of peptide substrates.

Here, using recombinant truncation variants that are sequentially lacking the individual helix and a flexible tail of mouse inducible Hsp72, we show the effect of deletion of the C-terminal domain on binding to two kinds of substrates with different peptide length.

2. Materials and methods

2.1. Materials

ATP-Na_2 (purity >98%), ATP-agarose (A-2767), and RCMLA were purchased from Sigma. Acrylodan-peptide CLLLSAPRR (a-p5) was synthesized at and purchased from Kurabo, BioMedical, Japan. The antiserum against mouse Hsp70 (SPA-812) from StressGen Biotechnologies Corp. (Canada) and the HRP-conjugated monoclonal antibody against histidine-tag from Invitrogen (Carlsbad, CA, USA) were used for detection of the recombinant variants. EZ-Link™ sulfo-NHS-LC-biotin (Pierce) was used to biotinylate the RCMLA protein. A fluorescein-EX labeling kit to fluoresceinate proteins was from Molecular Probe. Labeling of RCMLA was performed according to the manufacturer's protocol.

* Corresponding author. Fax: +81-774-33-3004 (or +81-774-38-3740).
E-mail address: tanifumi@kais.kyoto-u.ac.jp (F. Tani).

Abbreviations: RCMLA, reduced carboxymethyl α-lactalbumin

0014-5793/$22.00
doi:10.1016/j.febslet.2004.09.044

2.2. Cloning, expression, and purification of Hsp72 recombinant variants

To express mouse Hsp72 and its C-terminal truncation variants, d(1–615), d(1–562), d(1–543), and d(1–384), we introduced the corresponding cDNA fragments into pET-20b(+) vector using *Nde*I and *Xho*I sites (Novagen). Briefly, the corresponding cDNA fragments were amplified by PCR techniques using sets of specific primers and the plasmid mhsp72-pcDNA, which contains the cDNA encoding the entire sequence of mouse hsp72, as a template. 5′-GCACGAGGGATCCATATGGCCAAGAACACGGCGATC-3′ was used as the forward primer in all cases. The reverse primers for the wild-type, d(1–615), d(1–562), d(1–543), d(1–384) were 5′-CAGCAGAGGCTCGAGATCCACCTCCTCGATGGT-3′ for the full-length hsp72 with the entire sequence, 5′-TTTAGCCCCCTCGAGACCCGCACCCTGGTA-3′, 5′-GTCAGCCTCCTCGAGCTTGCCCTTGAGACC-3′, 5′-GAAGGCATAGGACTCGAGCGCGTTCTTGGC-3′, and 5′-CTGCACGTTCTCGAGCTTGTCCCCCATCAG-3′, respectively. These PCR products were subcloned into the same restriction enzyme sites of pET-20b(+). The resulting plasmids were suitable for expression of the designed proteins with a histidine tag at their C-termini. After the plasmids were introduced into *Escherichia coli* BL21(DE3), the bacteria harboring the constructed plasmids were grown in LB media for protein expression. After isopropyl-β-D-thiogalactopyranoside induction for 4 h, bacterial extract containing the designed proteins produced were applied to a Ni–NTA agarose (Qiagen) column, which was basically developed according to the manufacturer's protocol. After dialysis of the eluate against buffer A [20 mM HEPES, 20 mM KCl, 10 mM $(NH_4)_2SO_4$, 5 mM $MgSO_4$, 1 mM dithiothreitol, and 0.5 mM phenylmethylsulfonyl fluoride (pH 7.0)], the dialysate was applied to ATP agarose (Sigma), which was developed according to the method described by Schlossman et al. [22]. After extensive dialysis in the presence of EDTA and a saturated concentration of ammonium sulfate to remove ATP, all samples were finally dialyzed against buffer B [20 mM NaH_2PO_4, 150 mM KCl, and 3 mM 2-mercaptoethanol (pH 7.0)] and then stored at 4 °C before use.

2.3. Size-exclusion chromatography

The molecular size and status of recombinant proteins was analyzed by size-exclusion chromatography using a column of TSK gel G2000SW (7.5 i.d. × 300 mm, TOSOH, Tokyo, Japan) that was equilibrated with buffer C [20 mM NaH_2PO_4, 150 mM KCl (pH 6.5)]. The protein samples were incubated at 37 °C for 30 min in buffer B in advance and eluted with buffer C at a flow rate of 0.5 mL/min.

The size-exclusion chromatography with a column of Superdex 200 HR 10/30 (Amersham Biosciences, Piscataway, NJ, USA) was used to check complex formation of the truncation variants with the peptide a-p5. The proteins were eluted with buffer C at a flow rate of 0.5 mL/min and monitored at the wavelength of 280 nm. The acrylodan-derived fluorescence was detected using a spectrofluorometric detector RF-550 (Shimadzu, Kyoto, Japan) at the excitation wavelength of 370 nm and the emission wavelength of 520 nm.

2.4. Analyses of the binding of recombinant variants to peptide substrates

To measure complex formation of the recombinant proteins with the peptide a-p5, the excitation wavelength was set at 370 nm and the emission at 500 nm was recorded. The spectra of the peptide a-p5 or of the a-p5–protein complexes were scanned from 430 to 610 nm. Reactions were initiated by manually adding the peptide solution with a microliter pipette to protein solution in a quartz cuvette and observed at 25 °C for 30 min. The fluorescence spectral data were collected with a fluorescence spectrophotometer F-3000 (Hitachi, Japan).

FITC-labeled RCMLA was incubated at 37 °C for 30 min with the truncation variants at a molar ratio of 1:1 in the presence of buffer D [20 mM Tris–HCl, 150 mM KCl, and 3 mM 2-mercaptoethanol (pH 7.4)]. The variant-RCMLA complex was loaded on a column of TSK gel G3000SW (7.5 i.d. × 300 mm, TOSOH, Tokyo, Japan) that was equilibrated with buffer C. The proteins eluted were monitored at the wavelength of 280 nm and the FITC fluorescence was detected using a spectrofluorometric detector at the excitation wavelength of 492 nm and the emission wavelength of 515 nm.

The truncation variants were mixed with Ni–NTA magnetic beads (Qiagen) to immobilize the proteins through the C-terminal histidine-tag sequence. After 5 min of incubation, the immobilized proteins were incubated at 37 °C for 30 min with biotinylated RCMLA at a molar ratio of 1:1 in the presence of buffer E [10 mM NaH_2PO_4, 150 mM KCl, 3 mM 2-mercaptoethanol, and 0.005% Tween 20 (pH 7.5)]. After the incubation, the beads were washed twice with buffer E and then the variant–RCMLA complex was eluted from the beads in the presence of buffer F [50 mM NaH_2PO_4, 300 mM NaCl, 3 mM 2-mercaptoethanol, 250 mM imidazole, and 0.005% Tween 20 (pH 7.5)]. Eluted samples were subjected to SDS–PAGE and blotted onto PVDF membranes to detect the biotinylated RCMLA using a chemiluminescence system (Amersham Biosciences). To check the ATP-dependent dissociation of RCMLA substrate, the beads were treated at 37 °C for 5 min in the presence of 5 mM ATP and 10 mM $MgCl_2$ before washing the beads containing the variant–RCMLA complex.

2.5. CD measurement

CD spectra were recorded with a spectrometer (model J-720; Jasco, Tokyo Japan) equipped with an interface and computer. Far-UV CD spectra were recorded at a protein concentration of 0.25 mg/mL with a 1-mm cell at wavelengths from 250 to 195 nm. The unfolding transition curves for the recombinant proteins were obtained by measuring the ellipticity at 222 nm in a 1-mm cell at a protein concentration of 0.25 mg/mL in the presence of buffer B. The temperature was increased from 25 to 85 °C at a rate of 1.0 °C/min for the heat-denaturation process. The measured ellipticities were corrected for the temperatures monitored with a thermocouple (type SK-2000MC; Sato Keiryoki Mfg. Co., Ltd., Japan) and a flexible probe inserted directly into the 1-mm cell.

3. Results

3.1. Characterization of the recombinant truncation variants

The crystal structure of rat Hsc70 shows that its 10-kDa subdomain adopts a helix-loop-helix fold and that this con-

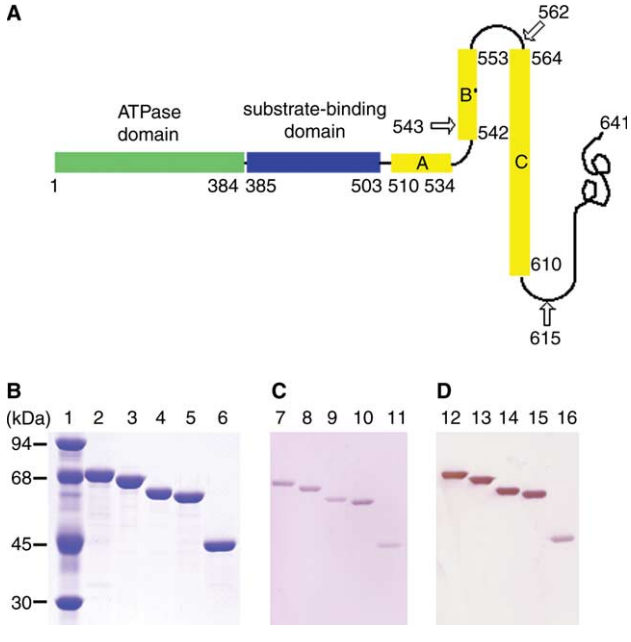

Fig. 1. Design of recombinant Hsp72 and its truncation variants. (A) Shown is a schematic of the wild-type Hsp72 (residues 1–641) with the boundaries indicated numerically. The lid region is not drawn to scale. (B) SDS–PAGE of the purified truncation variants. Samples (1.5 μg protein/lane) were electrophoresed on a 10% acrylamide gel and visualized by Coomassie Brilliant Blue staining: lane 1, molecular weight marker; lane 2, wild-type Hsp72; lane 3, variant d(1–615); lane 4, variant d(1–562); lane 5, variant d(1–543); lane 6, variant d(1–384). (C), (D) Western blotting of the purified truncation variants (150 ng protein/lane). Proteins were probed with polyclonal anti-Hsp72 antibody (C) and a monoclonal antibody against the histidine-repeat sequence (D): lanes 7 and 12, wild-type Hsp72; lanes 8 and 13, variant d(1–615); lanes 9 and 14, variant d(1–562); lanes 10 and 15, variant d(1–543); lanes 11 and 16, variant d(1–384).

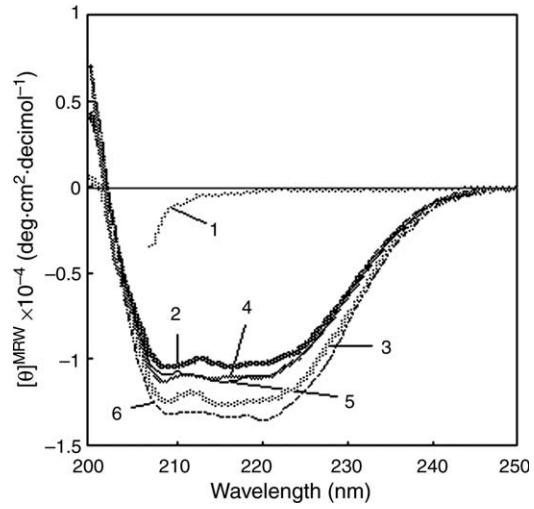

Fig. 2. Far-UV spectra of the recombinant proteins. Curve 1, Ovalbumin that had completely unfolded in the presence of 6 M guanidium hydrochloride; curve 2, wild-type Hsp72; curve 3, variant d(1–615); curve 4, variant d(1–562); curve 5, variant d(1–543); curve 6, variant d(1–384).

formation is different from the equivalent subdomain of DnaK, the bacterial homolog of Hsc70 [12]. Considering the data of Chou et al. showing that α-helix C corresponds to amino acid residues 564–610 in mouse inducible Hsp72, we designed recombinant variants that sequentially deleted the individual helices and the flexible tail (Fig. 1A). The variants d(1-615) and d(1–562) lack the flexible tail at the extreme C-terminus and the entire α-helix C, respectively. The variant d(1–543) was constructed as a protein containing the minimum unit of the substrate binding domain according to the data of Wang et al. [10]. The SDS–PAGE patterns showed that the purified proteins had the expected molecular sizes with purity over 98% (Fig. 1B). Western blotting patterns revealed that every product was reactive with the antiserum against Hsp70 and had a precise sequence at the C-terminus, confirming the structural integrity of the Hsp70 entity (Fig. 1C and D).

CD spectroscopy showed significant secondary structure in the truncation variants. Every variant showed significant and intrinsic secondary structure (Fig. 2). Especially, the profile of the wild-type protein had peaks at 208 nm and 222 nm, reflecting significant content of α-helix, whereas the profile of d(1–543), which lacks a few α-helices in the C-terminal 10-kDa subdomain, had the peak at 215 nm, suggesting the presence of significant β-sheet structure in the substrate binding domain.

3.2. Self-association of the recombinant truncation variants

Since several reports have shown that the C-terminal portion of Hsp70 molecules could be involved in self-association [12,23–25], the truncation variants were subjected to size-exclusion chromatography (Fig. 3). The wild-type recombinant and d(1–615) variant were found to exist as monomer, dimer and oligomer, although there may be differences in the proportions of self-association (Fig. 3A and B). On the other hand, variant d(1–562) predominantly existed as the monomer (Fig. 3C). The recombinant variants d(1–543) and d(1–384) were also monomeric (data not shown). This suggests that the long α-helix C at the C-terminus is responsible for self-association of Hsp70 molecules.

3.3. Thermal stability monitored by far-UV CD of the truncation variants

Fig. 4 shows the changes in the ellipticity at 222 nm of the truncation variants as a function of temperature in the range of 30–80 °C. The wild-type hsp72 (Fig. 4A) and d(1–615) variant (Fig. 4B) underwent a small cooperative conformational change in the vicinity of 42 °C followed by a second and less cooperative transition in the temperature range of 60–80 °C. Abrupt transition took place around the temperature of 42 °C for two truncation variants, d(1–562) and d(1–543) (Fig. 4C and D). In the presence of Mg^{2+}/ATP, however, the stability of all recombinant proteins was increased so that they were substantially stable at the temperature below 55 °C. Thus, the C-terminal truncation did not cause a marked decrease in thermal stability.

3.4. Molecular interactions between the truncation variants and various substrate peptides

A number of short peptides have been reported so far to bind to Hsp70, with K_d values ranging from 1 to 20 μM [13,16,26,27]. Unfolded proteins such as RCMLA and a

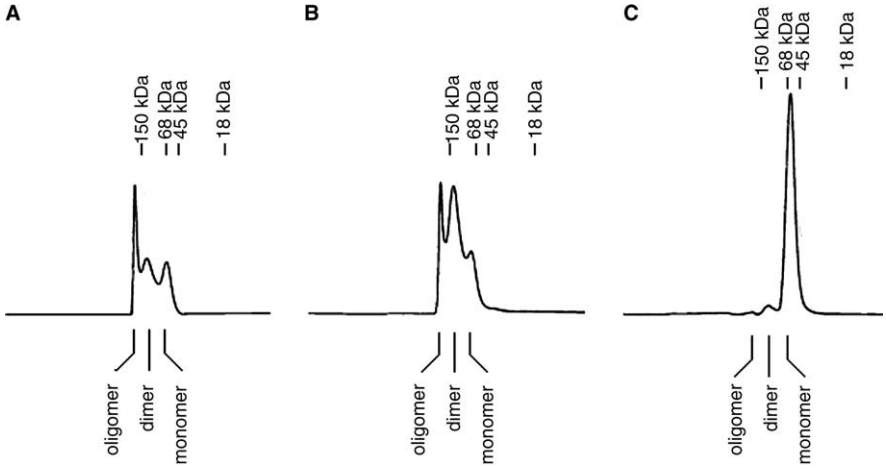

Fig. 3. Gel filtration analysis of the recombinant proteins. Gel filtration chromatography was performed as described in Section 2. Elution profiles are shown for the wild-type Hsp72 (A), variant d(1–615) (B), and variant d(1–562) (C).

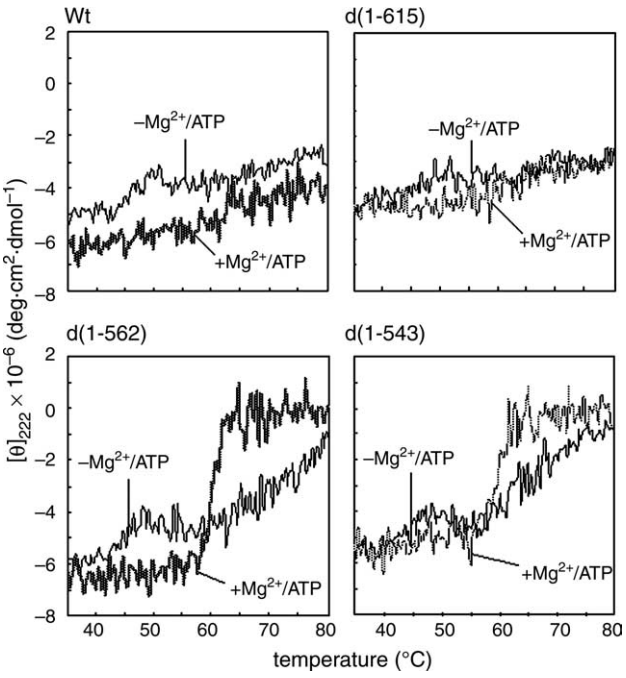

Fig. 4. Thermal stability monitored by far-UV CD of the truncation variants. Shown is the observed ellipticity at 222 nm that changes as a function of temperature. The temperature was increased from 25 °C to 85 °C at a rate of 1.0 °C/min for the heat-denaturation of the wild-type (A), variant d(1–615) (B), variant d(1–562) (C), and variant d(1–543) (D).

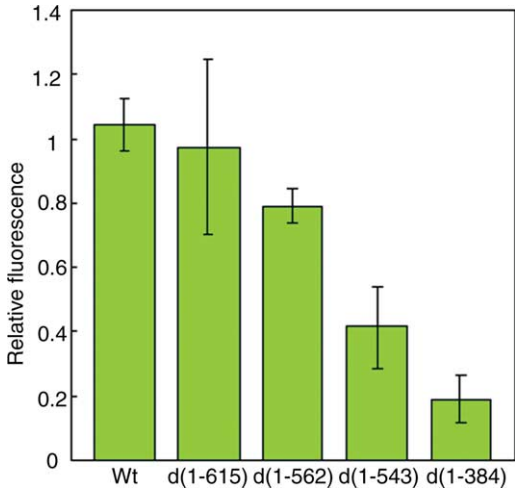

Fig. 5. Binding of acrylodan-CLLLSAPRR (a-p5) peptide to the recombinant proteins. Fluorescence emission spectra of protein-bound a-p5 were recorded under the conditions described in Section 2. The emission at 500 nm was compared as the relative fluorescence.

thermally unstable mutant of staphylococcal nuclease are also known to form complexes with Hsp70 [17–19]. We investigated if the types of peptide substrate may affect the binding properties of Hsp72. The peptide a-p5 is a representative substrate for *E. coli* Hsp70 DnaK [28–30]. On binding to DnaK under our experimental conditions, the fluorescence spectrum of a-p5 underwent a blue shift of emission maximum from 526 to 513 nm, depending on the concentration of DnaK. The fluorescence intensity of a-p5 at 500 nm in the presence of 10 μM DnaK concomitantly increased to 370% of that of the unbound ligand (data not shown). When the relative fluorescence of a-p5 as a measure of peptide binding was compared among the truncation variants at the concentration of 10 μM (Fig. 5), the variants containing substrate-binding domain displayed significant binding of the peptide a-p5. Binding of the peptide a-p5 by the truncation variants including d(1–562) was clearly detected by the size-exclusion chromatography as shown in Fig. 6. We observed the decreased fluorescence intensity in both experiments by sequentially deleting the C-terminal region of Hsp72. This may result from increased quenching that is expected as the lid structure is deleted. However, these data suggest that the truncation variants intrinsically retain the ability to bind peptide substrate.

When the formation of substrate–Hsp72 complex was examined using an unfolded protein RCMLA instead of the nonapeptide a-p5, FITC-labeled RCMLA bound the wild-type Hsp72 and variant d(1–615) (Fig. 7A and B). Addition of Mg^{2+}-ATP to the reaction mixture caused dissociation of the RCMLA substrate from Hsp72 complexes (Fig. 7D and E), suggesting that the substrate binding was intrinsically ATP-dependent. In this gel filtration experiment, however, we could not observe the peak showing the complex of other shorter truncation variants such as variant d(1–562) with RCMLA (Fig. 7C). To address if protein stability can affect the binding property, we examined the binding of d(1–562) variant with RCMLA in the presence of Mg^{2+}/ADP. No detectable peak appeared under this condition, as shown in Fig. 7F.

Then, we examined binding property of the truncation variants to RCMLA substrate under the condition where they were immobilized on the Ni^{2+}–NTA magnetic beads through

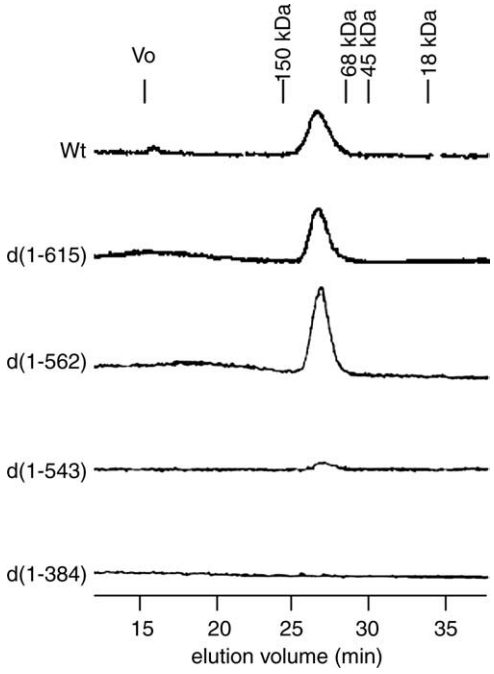

Fig. 6. Gel filtration analysis of the recombinant proteins complexed with a-p5 peptide. Gel filtration chromatography was performed as described in Section 2. From upper line, elution profiles are shown for the wild-type Hsp72, variant d(1–615), variant d(1–562), variant d(1–543), and variant d(1–384).

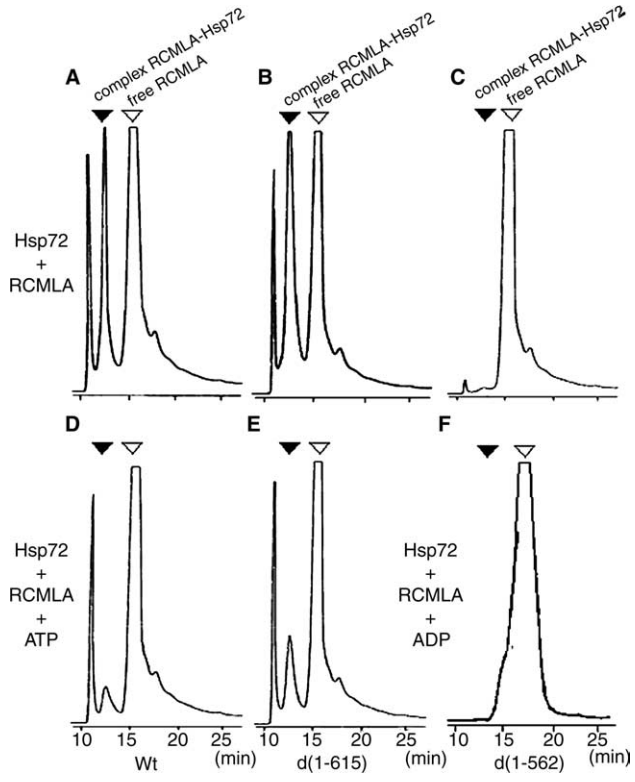

Fig. 7. Binding of FITC-labeled RCMLA to the recombinant proteins free in solution. Gel filtration chromatography was performed as described in Section 2. The upper three panels show the elution profiles of FITC-labeled RCMLA that was mixed with wild-type Hsp72 (A), variant d(1–615) (B), and variant d(1–562) (C). The lower three panels show the elution profiles of the wild-type Hsp72 (D) and d(1–615) variant (E) after incubation in the presence of Mg^{2+}/ATP, and d(1–562) variant after incubation in the presence of Mg^{2+}/ADP (F). Elution positions of the complex RCMLA-Hsp72 and free RCMLA are shown by closed and open triangles, respectively.

the interaction with the C-terminal histidine tag sequence. As shown in Fig. 8, the variants except for d(1–384) showed nucleotide-dependent formation of the Hsp-RCMLA complexes,

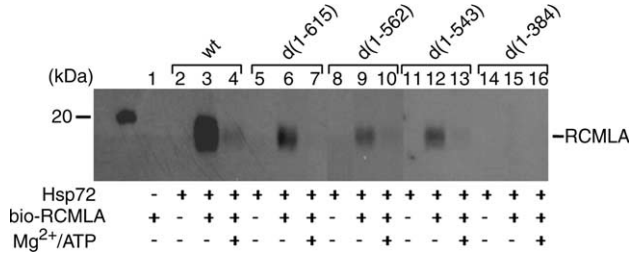

Fig. 8. Binding of biotinylated RCMLA to the recombinant proteins anchored onto Ni-NTA solid phase. Biotinylated RCMLA that had bound to wild-type Hsp72 and its truncation variants was analyzed by SDS–PAGE and visualized using the ECL Western blotting analysis system (Amersham) with HRP-conjugated streptavidin. No RCMLA was detected in the reaction without Hsp72 (lane 1). The wild-type Hsp72 (lanes 2–4), variant d(1–615) (lanes 5–7), variant d(1–562) (lanes 8–10), variant d(1–543) (lanes 11–13), or variant d(1–384) (lanes 14–16) was incubated in the absence (lanes 2, 5, 8, 11, and 14) or the presence (lanes 3, 4, 6, 7, 9, 10, 12, 13, 15, and 16) of biotinylated RCMLA. The reaction mixtures were treated with ATP to dissociate the Hsp70-RCMLA complex (lanes 4, 7, 10, 13, and 16).

although there may have been differences in the binding capacity. Interestingly, unlike the case of the peptide a-p5, the deletion of the flexible tail portion greatly reduced the ability of the truncation variants to bind to RCMLA.

4. Discussion

In the present study, we showed that the long α-helix C in the helical lid and the following flexible region of Hsp72 influence the recognition of a large mass substrate. The kinetics for substrate release may be substrate-mass dependent. Also, helix C was shown to be required for self-association of Hsp72.

The truncation variants containing the substrate-binding domain were shown to bind a short-length peptide a-p5 (see Figs. 5 and 6). Taking into account quenching effect, the observed decrease in fluorescence does not always reflect a decrease in the amount of bound peptide. However, we qualitatively showed that residues 385–543 in the variants we produced can form a functional subdomain that potentially has binding ability for the substrate peptide. This observation is compatible with the report of Wang et al. [10].

When RCMLA was used as a large mass substrate, we could not detect the peak showing the complex of the variant d(1–562) with RCMLA in the size-exclusion chromatography experiment. In contrast, d(1–562) variant was shown to bind RCMLA when the variant was immobilized on the Ni^{2+}–NTA magnetic beads. This discrepancy may be explained by the following possible reasons. First, the β-sandwich substrate-binding domain itself may have lost the structural stability needed for recognition of RCMLA polypeptide because, in general, the truncation causes the decrease in protein stability to change physical properties. However, a marked decrease in thermal stability by the C-terminal truncation was not observed as shown in Fig. 4. There was no peak showing the complex of d(1–562) variant with RCMLA even though the stability of the variant was increased in the presence of Mg^{2+}/ADP. These data allow us to rule out the first possibility.

Second, d(1–562) variant could bind RCMLA, but the off-rate has increased compared to the wild-type. RCMLA might dissociate from the variant during the transit time down the column of gel filtration, because helix D in DnaK was shown to be essential for long-lived DnaK-peptide complexes and the off-rate was markedly increased when helix D is deleted [31]. The region equivalent to helix D of DnaK is included in the sequence between 563 and 615 residues of mouse Hsp72. Taking into account that the complex of d(1–562) variant with a-p5 peptide was clearly detected in the column experiment as shown in Fig. 6, this observation raises the possibility that the increase in off-rate can be substrate-mass dependent. To address this problem, we should require a larger set of quantitative experiments with peptide libraries showing diversity in sequence and mass.

An individual helix in the C-terminus of DnaK discretely coordinates the functional structure of the helical lid of DnaK. Helix D of DnaK is necessary and sufficient to create the protective lid structure when a substrate peptide is added. In the absence of peptide, helix E promotes the formation of the antiparallel helical bundle composed of the B to D helices and prevents internal ligand formation [31]. Wang and colleagues showed that internal ligand formation, i.e., self-binding, occurs in the region of DnaK which contains the β-sandwich sub-

strate-binding domain plus the lid helices αA and αB [32]. This self-binding results from the fact that leucine residue 543 in helix B is tightly held in a deep hydrophobic pocket within the substrate-binding site, leading to stabilization of substrate-binding domain. Similarly, in rat Hsc70, leucine residue 542 was observed to intramolecularly interact with the hydrophobic groove of the substrate-binding domain by salt-bridge formation [33]. Three discrete helices C-E in DnaK are equivalent to the long α-helix C in the helix-loop-helix fold of rat Hsc70 [12]. Assuming that the C-terminal structure of mouse inducible Hsp72 is similar to that of the rat Hsc70 homolog, the region around the end of helix B′ of variant d(1–562) is presumed to cause internal ligand formation that retards RCMLA recognition. The long helix C of mouse Hsp72, which contains the equivalent portion to helices D and E of DnaK, may regulate internal ligand formation by helix B′. According to the substrate mass, therefore, helix C may play a role in modulating the off-rate for substrate binding.

Another interesting result in this study is that deletion of the flexible tail results in decreased RCMLA binding (see Fig. 8). Recently, Demand et al. reported that the C-terminal 10-kDa domain could interact with Hdj-1/Hsp40 [34]. The EEVD motif at the extreme C-terminus of human Hsp70, which is conserved among many species, is known to be important for its peptide binding activity and ATPase activity because mutation of the EEVD sequence abolishes chaperone activity [35,36]. The reduction of RCMLA binding to d(1–615) variant, compared to the wild-type Hsp72, might result from the deletion of this EEVD motif in the variants. Deletion of the lid of DnaK increases the kinetics of ATP-triggered peptide release [37]. The flexible tail and helix E of DnaK modulate the kinetics of ATP binding [31]. Taken together, the C-terminal tail could work in concert with the nucleotide-binding domain to control the kinetics for binding of a large mass substrate.

Additionally, our present data clearly showed that helix C dictates the chaperone self-association (see Fig. 4) and are thus compatible with the results reported by Chou et al. [12]. Under certain conditions Hsp70 proteins are known to exist as oligomers, which are converted to monomers in the presence of peptide substrates or ATP [17,38]. That oligomers also form in vivo has been suggested by genetic data obtained from studies of dominant hsp70 mutations and intergenic complementation experiments between hsp70 mutants [39,40].

Considering that the C-terminal region of Hsp70 may modulate the kinetics of the substrate recognition according to the substrate-mass specific off-rate, we speculate that the helical lid region of Hsp70 may significantly regulate intracellular protein synthesis as the chain length of a polypeptide being synthesized increases. Further investigations will be needed in the future to elucidate the biological function of the C-terminal region of the Hsp70 family in vivo.

Acknowledgements: This work was supported in part by a Grant-in-Aid for Scientific Research (C) (No. 12660076) and a Grant-in-Aid for Exploratory Research (No. 15658108) to F. T. from the Ministry of Education, Science, Sports, and Culture of Japan.

References

[1] Ellis, R.J. and van der Vies, S.M. (1991) Annu. Rev. Biochem. 60, 321–347.
[2] Gething, M.-J.H. and Sambrook, J.F. (1992) Nature 355, 33–45.
[3] Hartl, U.F. (1996) Nature 381, 571–580.
[4] Bukau, B. and Horwich, A.L. (1998) Cell 92, 351–366.
[5] Rüdiger, S., Buchberger, A. and Bukau, B. (1997) Nat. Struct. Biol. 4, 342–349.
[6] Chappell, T.G., Konforti, B.B., Schmid, S.L. and Rothman, J.E. (1987) J. Biol. Chem. 262, 746–751.
[7] Flaherty, K.M., DeLuca-Flaherty, C. and McKay, D.B. (1990) Nature 346, 623–628.
[8] Flaherty, K.M., McKay, D.B., Kabash, W. and Holmes, K. (1991) Proc. Natl. Acad. Sci. USA 88, 5041–5045.
[9] Bork, P., Sander, C. and Valencia, A. (1992) Proc. Natl. Acad. Sci. USA 89, 7290–7294.
[10] Wang, T.-F., Chang, J.-H. and Wang, C. (1993) J. Biol. Chem. 268, 26049–26051.
[11] Zhu, X., Zhao, X., Burkholder, W.F., Gragerov, A., Ogata, C.M., Gottesman, M.E. and Hendrickson, W.A. (1996) Science 272, 1606–1614.
[12] Chou, C.-C., Forouhar, F., Yeh, Y.-H., Shr, H.-L., Wang, C. and Hsiao, C.-D. (2003) J. Biol. Chem. 278, 30311–30316.
[13] Flynn, G.C., Chappell, T.G. and Rothman, J.E. (1989) Science 245, 385–390.
[14] Beckman, R.P., Mizzen, L.A. and Welch, W.J. (1990) Science 248, 850–854.
[15] Flynn, G., Pohl, J., Flocco, M. and Rothman, J. (1991) Nature 353, 726–730.
[16] Blond-Elguindi, S., Cwirla, S., Dower, W., Lipshutz, R., Sprang, S., Sambrook, J. and Gething, M.-J. (1993) Cell 75, 717–728.
[17] Palleros, D.R., Welch, W.J. and Fink, A.L. (1991) Proc. Natl. Acad. Sci. USA 88, 5719–5723.
[18] Palleros, D.R., Shi, L., Reid, K.L. and Fink, A.L. (1994) J. Biol. Chem. 269, 13107–13114.
[19] Sadis, S. and Hightower, L.E. (1992) Biochemistry 31, 9406–9412.
[20] Rüdiger, S., Germeroth, L., Schneider-Mergener, J. and Bukau, B. (1997) EMBO J. 16, 1501–1507.
[21] Hu, S.-M. and Wang, C. (1996) Arch. Biochem. Biophys. 332, 163–169.
[22] Schlossman, D.M., Schmid, S.L., Braell, W.A. and Rothman, J.E. (1984) J. Cell Biol. 99, 723–733.
[23] Wilbanks, S.M., Chen, L., Tsuruta, H., Hodgson, K.O. and McKay, D.B. (1995) Biochemistry 34, 12095–12106.
[24] Benaroudj, N., Fouchaq, B. and Ladjimi, M.M. (1997) J. Biol. Chem. 272, 8744–8751.
[25] Fouchaq, B., Benaroudj, N., Ebel, C. and Ladjimi, M.M. (1999) Eur. J. Biochem. 259, 379–384.
[26] Tsai, M.-Y. and Wang, C. (1994) J. Biol. Chem. 269, 5958–5962.
[27] Terlecky, S.R., Chiang, H.-L., Olson, T.S. and Dice, J.F. (1992) J. Biol. Chem. 267, 9202–9209.
[28] Schmid, D., Baici, A., Gehring, H. and Christen, P. (1994) Science 263, 971–973.
[29] Pierpaoli, E.V., Sandmeier, E., Baici, A., Schönfeld, H.-J., Gisler, S. and Christen, P. (1997) J. Mol. Biol. 269, 757–768.
[30] Pierpaoli, E.V., Gisler, S. and Christen, P. (1998) Biochemistry 37, 16741–16748.
[31] Slepenkov, S.V., Patchen, B., Peterson, K.M. and Witt, S.N. (2003) Biochemistry 42, 5867–5876.
[32] Wang, H., Kurochkin, A.V., Pang, Y., Hu, W., Flynn, G.C. and Zuiderweg, E.R.P. (1998) Biochemistry 37, 7929–7940.
[33] Morshauser, R.C., Hu, W., Wang, H., Pang, Y., Flynn, G.C. and Zuiderweg, E.R.P. (1999) J. Mol. Biol. 289, 1387–1403.
[34] Demand, J., Luders, J. and Hohfeld, J. (1998) Mol. Cell. Biol. 18, 2023–2028.
[35] Boorstein, W.R., Ziegelhoffer, T. and Craig, E.A. (1994) J. Mol. Evol. 38, 1–17.
[36] Freeman, B.C., Myers, M.P., Schumacher, R. and Morimoto, R.I. (1995) EMBO J. 14, 2281–2292.
[37] Slepenkov, S.V. and Witt, S.N. (2002) Biochemistry 41, 12224–12235.
[38] Blond-Elguindi, S., Fourie, A.M., Sambrook, J.F. and Gething, M.-J.H. (1993) J. Biol. Chem. 268, 12730–12735.
[39] Nicolet, C. and Craig, E. (1991) Yeast 7, 699–716.
[40] Wild, J., Kamath-Loeb, A., Ziegelhoffer, E., Lonetto, M., Kawasaki, Y. and Gross, C.A. (1992) Proc. Natl. Acad. Sci. USA 89, 7139–7143.